ELSEVIER

Chemical Physics 228 (1998) 241–253

Chemical Physics

Structural and dynamical properties of HCl dissolved in CCl_4. A molecular dynamics study

G. Chatzis, M. Chalaris, J. Samios *

University of Athens, Department of Chemistry, Laboratory of Physical Chemistry, Panepistimiopolis, Athens 157-71, Greece

Received 7 August 1997; accepted 3 November 1997

Abstract

Molecular dynamics simulation was used to study the local structure and the single-molecule dynamical properties of HCl dissolved in liquid CCl_4. The intermolecular interactions between solute and solvent molecules were investigated and an accurate effective potential model was proposed. The local structure of HCl in the solution is well described in terms of the calculated relevant pair distribution functions. The linear and angular velocity, the torque and the center of mass total force, as well as the first- and second-order reorientational autocorrelation functions (ACFs) have been obtained and discussed. Finally, this study has shown that on the basis of the proposed potential the predicted rotational dynamics of the solute molecule are in successful agreement with experimental infrared results reported in the past. © 1998 Elsevier Science B.V.

1. Introduction

The dense phase of relative simple molecules solved in non-polar solvents has been extensively studied for many years. Much has been learned about the dynamics of the solute molecules perturbed by the non-polar solvents from experimental [1–5], theoretical [6,7], and computer simulation (CS) [8–11] studies. More recently, there has been a renewed interest in the investigation of such systems. The reason for this is that many questions concerning the properties of these systems remain to be answered.

Hydrogen chloride (HCl) is a representative heteronuclear, quite small diatomic molecule. It has relatively large dipole ($\boldsymbol{\mu}$) and quadropole ($\boldsymbol{Q}$) moments as well as a moderate polarizability ($\boldsymbol{\alpha}$). The properties of the pure system in the gas and condense phase have been the subject of a body of experimental [12–16] and computational [17–22] work, far too extensive to review in the present study. Moreover, the solutions of HCl in non-polar solvents have aroused wide interest and several spectroscopic studies have been reported. An interesting feature that characterizes the infrared (IR) spectral lineshapes of HCl in solutions, is that in addition to the Q branch, the P and R branches are also observed. The appearance of these bands is clear evidence that HCl in solution possesses the ability to execute relatively free rotational motion.

In recent years the dynamics of HCl in liquid CCl_4 have been studied experimentally and a num-

* Corresponding author.

PII S0301-0104(97)00338-8

ber of spectroscopic studies have been reported by several groups. Thus, spectroscopic studies, such as far-infrared (FIR) [23–25], IR [4,26,27] and isotropic Raman [28,29], have provided interesting information about this molecular system. In addition, some theoretical efforts have been concentrated on the analytical evaluation of the FIR and IR relevant correlation functions and the corresponding absorption coefficients. Kolmykov and McConnel [30] have proposed an extended *J*-diffusion model based on the Zwanzig–Mori formalism [31,32]. In this treatment inertial effects as well as a finite time of the molecular collisions have been taken into account. This generalized model has been applied to the experimental FIR absorption of HCl in cyclohexane [33], HCl in CCl_4 [23–25] and DCl in SF_6 [2]. The authors pointed out that the model parameters obtained are in accordance with the previous reports [24,34]. In the case of IR spectra of HCl in CCl_4, Carlier and Turrell [35] proposed an interpretation based on an analytical model of hindered rotation motion of the solute within a cage of solvent molecules. Although this model is developed in one dimension and neglects long-range forces, it provides results which are considered to be satisfactory compared with the observed absorption profiles. Note however that a more realistic model of this type in three dimensions is not available in the literature. More recently, some dynamical properties of HCl dissolved in CCl_4 have been obtained from molecular dynamics (MD) simulations by Idrissi et al. [36]. In this MD study various site–site potential models were used for the description of the intermolecular interactions. The reorientational first-order autocorrelation function (RACF) $C_1(t)$ of HCl has been calculated and compared with the experimental ACF obtained from the band shape analysis of the IR spectra. The authors concluded that the employed interaction potential models yield good agreement at both short and long times with the experimental CFs. However, at intermediate times the characteristic minimum and submaximum observed in the experimental CF are not reproduced. They made the assumption that this observed feature 'may well be' due to the induction effects between solute and solvent molecules. These effects were not investigated in this previous MD study.

In view of this situation, we decided to continue the work on this field by performing an extensive MD study of this solution. In the framework of the present study, the intermolecular interactions are reinvestigated and a new potential model is proposed. Particular attention has been paid to the anisotropic interactions between the solute and the highly symmetric solvent molecules. Moreover, the intermolecular structure between the solute and its surrounding solvents, as well as the molecular motion, has been studied in detail. Note also that the main purpose of the present paper is to investigate the dynamical properties of the molecules in the solution with special emphasis on the rotational dynamics of the solute molecules. For this purpose the most important ACFs have been obtained and compared with available experimental data. Finally, the procedure and results of this MD study are presented herein.

2. Potential model and simulation details

2.1. Potential model

Following the literature, we can see that both pure substances have received much attention in MD simulation studies at liquid densities. In these studies the most common proposed anisotropic pair potentials were of the type site–site pair-wise additive, containing short-range Lennard-Jones (LJ) and long-range Coulombic terms [17–22,37,38]

$$U(r_{ij}) = \sum\sum \left\{ 4\epsilon_{ij} \left[\left(\frac{\sigma_{ij}}{r_{ij}} \right)^{12} - \left(\frac{\sigma_{ij}}{r_{ij}} \right)^{6} \right] + \frac{q_i q_j}{4\pi\epsilon_0 r_{ij}} \right\}. \quad (1)$$

In Eq. (1) the sums are over all pairs of interactions sites *ij* located on different molecules. q_i and q_j denote the partial local charges and r_{ij} is the distance between two interaction sites.

It is also interesting to note that in two successful MD simulation studies of liquid HCl the proposed site–site potential model was of the type exp − 6 with electrostatic terms [19,22].

As mentioned above, only one MD simulation study of this solution has been reported up to date [36]. In this treatment various potential models have been employed for the CCl_4–CCl_4, HCl–HCl and HCl–CCl_4 interactions in the system. However, the predicted rotational dynamics are considered to be not satisfactory compared with the experimental results. At this stage, we decided to construct a new potential model for the description of the intermolecular interactions between the various species in the solution. This work was particularly extensive covering various types of potential models which were tested by numerous MD runs. Thus, in the frame work of this study, a new optimized effective potential model for this solution has been evaluated. The model details are presented below and the various model parameters are summarized in Table 1.

According to this model, for the CCl_4–CCl_4 interactions we have employed a 5-site LJ (12-6) pair-wise additive potential, plus charge–charge electrostatic terms. The charges coincide with the LJ centers located at the nuclei of the five atoms of the molecule. On the basis of this charge distribution the calculated octopole moment of CCl_4 corresponds to the value of 15 D Å^2 [20].

On the other hand, the HCl–HCl interactions were represented by a 2-site LJ (12-6) model with charge–charge electrostatic interactions. Here we have adopted a local charge distribution for HCl which has been previously used by Laaksonen and Westlund [22] in their MD simulation study of this liquid. The fractional charges are distributed by placing a positive charge $q_H = 0.4\,e$ on the H atom, a negative charge $q_{Cl} = -0.8\,e$ on the Cl atom and finally, a third positive charge $q_D = 0.4\,e$ outside the bond length d_{H-Cl} and at a distance of 0.6 Å from the site of the Cl atom. This model produces an effective dipole moment for this molecule which is slightly enhanced compared to the experimental value. Note that the reason for using an enhanced dipole moment in modeling molecular liquids generally is to account for the mutual polarization of the neighbor molecules.

Finally, for the most significant of the solute dynamics HCl–CCl_4 interactions, among the various intermolecular pair potentials that have been tested here, we have chosen the one that, in connection with the above described solvent–solvent and solute–solute models, gives the best agreement with experimental data from spectroscopic measurements.

Table 1
Potential model and parameter values for the HCl–CCl_4 solution

	Type of interaction	Site	ϵ (K)	σ (Å)	q (e)
CCl_4–CCl_4	LJ + Coulomb	C	51.2	4.60	+0.552
		Cl	102.4	3.50	−0.138
			$r_{C-Cl} = 1.766$ Å		
HCl–HCl	LJ + Coulomb	H	19.4	2.50	+0.400
		Cl	173.4	3.35	−0.800
		q_D			+0.400
		$r_{H-Cl} = 1.270$ Å	$r_{Cl-q} = 0.600$ Å	$r_{H-q} = 1.870$ Å	

		CCl_4 site	HCl site	A (eV)	ρ (Å)	C (eV Å^6)
CCl_4–HCl	exp − 6 + Coulomb	Cl	Cl	8550.2	0.2801	67.529
		C	Cl	7972.7	0.3177	115.004
		Cl	H	3297.3	0.2195	10.67
		C	H	11661.2	0.2504	17.089
			charges as before			

The cross LJ interaction parameters are obtained using the Lorentz–Berthelot mixing rules.

This is a site–site pair-wise additive potential of the type exp − 6 with charge–charge electrostatic interactions

$$U(r_{ij}) = \Sigma\Sigma\left[A_{ij} \exp\left(-\frac{r_{ij}}{\rho_{ij}} \right) - \frac{C_{ij}}{r_{ij}^6} \right] + \Sigma\Sigma \frac{q_i q_j}{4\pi\epsilon_0 r_{ij}} . \quad (2)$$

The short-range interaction sites are located on the atoms of the molecules. The exact positions of the fractional charges on the HCl and CCl_4 molecules are described above.

2.2. Technical details

The MD simulations were carried out in microcanonical ensemble (NVE) with 2 solute molecules dissolved in 254 CCl_4 solvents in a cubic box with periodic boundary conditions. In order to check the reliability of the predicted results, we have performed some supplementary MD runs with 4 solutes in 496 solvent molecules. It should, however, be noted that no significant differences in the results have been observed. The direct Ewald summation method was used to treat the long-range Coulombic interactions. The system was simulated at 293 K and corresponding density for which experimental data from spectroscopic studies are available. The molecules are treated as rigid rotators. The geometrical characteristics of the molecules are given in Table 1 and the permanent multipole moments and polarizabilities of the molecules are summarized in Table 2.

The orientation of the molecules have been formulated using a quaternion interpretation which offers the possibility the equations of motions to be free of singularities. The translational and rotational equations of motions are solved using leapfrog algorithms. In order to achieve the best stability of the results, we have tested several integration time steps Δt. By comparing the predicted results we were able to conclude that a time step of 2×10^{-15} s insures stability of the calculated energy and momentum. Each MD run was started from a FCC structure and the number of equilibration time steps was between 30 000 and 50 000. In order to obtain accurate statistics the production runs were extended approximately to 300 ps and some of them to 500 ps. It was necessary due to the small number of the HCl molecules in the sample.

Finally, the calculated macroscopical properties are selected in Table 3.

Table 2
Multipole moments and polarizabilities of HCl and CCl_4 used in the present study

Molecule	μ (D)	Q (D Å)	Ω (D Å^2)	α (Å^3)	γ (Å^3)
HCl	1.29 (1.01)	3.83 (3.74)	3.2 (2.4–4.5)	2.60	0.311
CCl_4	0	0	15	11.2	0

The numbers in parentheses denote Exp./Theor. values from appendix D of Ref. [39].

3. Results and discussion

3.1. Macroscopical properties

Table 3 contains the simulated mean potential energy U and pressure P as well as the translational diffusion coefficients of the molecules in the solution. The system was equilibrated at 290 K and the fluctuation of the temperature was ± 3 K. The numbers in parentheses denote experimental data of the pure liquid CCl_4. From the data in this table we may conclude that the agreement between MD results and the corresponding experimental values of these thermodynamic properties is quite satisfactory at this thermodynamic point. Unfortunately, experimental values for the self-diffusion coefficients of HCl in CCl_4 are not available in the literature. Therefore, a direct comparison between the predicted MD diffusion coefficients and experiment is not possible. However, by taking into account the sizes and weights of the solute and solvent molecules, we can see that the obtained diffusion values are realistic compared to the corresponding experimental diffusion coefficients of other similar molecular liquids.

The root-mean-square (rms) force $\langle \boldsymbol{F}^2 \rangle^{1/2}$ and torque $\langle \boldsymbol{T}^2 \rangle^{1/2}$ acting on the solute due to its surrounding solvent molecules are calculated and the

Table 3
MD results for the solution HCl–CCl_4 (mole fraction of HCl: 0.008)

Number of molecules HCl in CCl_4	V_m	T	U_{pot}	P	D_{HCl}	D_{CCl_4}
	(cm^3)	(K)	(kJ/mol)	(kbar)	(10^{-9} m^2/s)	(10^{-9} m^2/s)
2:254	96.5	290	−32.335	−0.033	3.91	1.44
			(−32.20)	(0.0001)	3.68[a]	(1.40)

Depicted are the molar volume V_m and the equilibrium properties: temperature, T; potential energy, U_p; pressure, P; and the calculated translational diffusion coefficients of both species. The numbers in parentheses are the experimental data of pure liquid CCl_4 [40–42].
[a] From [36].

obtained results are displayed in Table 4. Results for these properties have been also reported in the previous MD study of this solution. Moreover, these properties have been estimated from the second and fourth moments of the IR spectral profile [27]. This estimation was based on theoretical expressions, whose derivations involve a number of approximations [26]. Thus, the experimentally estimated value for the rms force and torque on the solute is 2.97×10^{11} cm^{-2} and 371 cm^{-1}, respectively, at this temperature. It should be noted that due to the experimental errors the rms torque can, in principle, be determined from the bandshapes with an accuracy of $\sim 15\%$ or better [43]. Although one finds that the simulated rms torques deviate by at least one order of magnitude from the experimental values, the data in Table 4 show that the agreement between the rms torque from this work and from experiment is remarkably good.

3.2. Intermolecular structure

The intermolecular structure of the simulated system is presented in the form of the pair correlation functions (PCFs). Due to the dilution of HCl in CCl_4 the PCFs of interest are the following:

(i) the COM functions between HCl (a) and CCl_4 (b) and between CCl_4 molecules, namely $G_{a-b}(r)$, $G_{b-b}(r)$, and

(ii) the four atom–atom PCFs $G_{H(a)-Cl(b)}(r)$, $G_{H(a)-C(b)}(r)$, $G_{Cl(a)-Cl(b)}(r)$ and $G_{Cl(a)-C(b)}(r)$ between the atoms of the solute and the atoms of the solvent. All these functions have been calculated and their characteristic extrema as well as the obtained average coordination numbers are summarized in Table 5. These functions are also displayed in Fig. 1a–c.

Unfortunately, information regarding the structure of HCl in liquid CCl_4 from X-ray and neutron diffraction experiments is not available in the literature. The only available results are those reported in the previous MD simulation. Therefore, at this state no more definitive answer to this problem can be given, and discussion is limited to a comparison of our results with those obtained on the basis of the model III used in [36].

As we can see in Fig. 1a, the first peak of the solute–solvent COM PCF $G_{a-b}(r)$ is located at

Table 4
Correlation times τ_c (ps) of the linear velocity u, angular velocity ω, center of mass total force $\boldsymbol{F}$, torque $\boldsymbol{T}$, P_1 and P_2 Legendre polynomials ACFs and the rms force and torque of the HCl molecule

	$\langle \boldsymbol{T}^2 \rangle^{1/2}$ (cm^{-1})	$\langle \boldsymbol{F}^2 \rangle^{1/2}$ (10^{11} cm^{-2})	τ_u	τ_ω	τ_F	τ_T	τ_{P_1}	τ_{P_2}
This work	480.8	1.51	0.056	0.144	0.001	0.001	0.190	0.086
MD [36]	742.0	1.62	0.055	0.034	0.0036	0.0024	0.218	
Exp. [27,43]	371.0	2.97	–	–	–	–	0.189	

Table 5
Positions and heights of the first maximum and minimum in the calculated PCFs (r(Å):$G(r)$) and the coordination numbers obtained for the first shell around the solute molecule

$G(r)$	I. maximum		I. minimum		Coord. number	
	posit. (Å)	ampl.	posit. (Å)	ampl.	I. max.	I. min.
COM(a)–COMb)	4.60	2.26	6.80	0.586	2.185 (3.7)[a]	8.63
COM(b)–COM	5.60	2.266	8.0	0.592	3.23	13.17
Cl(a)–C(b)	4.60	2.258	6.80	0.593	2.185 (3.8)[a]	8.637
H–C(b)	4.40	1.79	7.00	0.723	1.916 (4.2)[a]	9.18
Cl(a)–Cl(b)	3.60	1.883	5.00	0.876	2.92	12.95
H–Cl(b)	4.80	1.208	7.00	0.906	11.15	36.0
Plateau on the	3.00	0.947	–	–	1.42	–
$G_{\mathrm{H-Cl}(b)}(r)$	3.60	0.934	–	–	3.43	–

[a]The number in parentheses denote the coordination numbers up to the shoulders.

shorter distance than the first peak of the solvent–solvent $G_{b-b}(r)$ function. This is in agreement with the size/shape of the two-component molecules in the solution. Note also that these functions are found to be in good agreement with those reported in the previous MD study. In addition, concerning the HCl–CCl_4 PCF we observe a small shoulder on the right-hand side of the first peak. This feature reflects clearly the anisotropic shape of the HCl molecule and suggests the existence of a local structure between the solute and the nearest solvent molecules. The coordination number up to the first minima in $G_{a-b}(r)$ is about 8 or 9 CCl_4 molecules. However, the number of the nearest solvent molecules around the solute molecule is about 2, or maximal 4. These coordination numbers have been obtained by integrating the solute–solvent PCF up to the first peak (4.60 Å) and up to the observed shoulder (5.1 Å), respectively.

In order to study the local structure around the solute molecule in detail, it is necessary to examine the site–site PCFs between the solute and the solvent atoms. These functions are presented in Fig. 1b and c. As expected, due to position of the Cl atom relative to the COM of the HCl molecule, the Cl(a)–C PCF is very similar to the above discussed COM–COM HCl–CCl_4 PCF. On the other hand, the H–C PCF shows some interesting features. For example, the first peak in this function is located at a shorter distance than the first peak in the corresponding function obtained on the basis of the potential models in [36]. Note also that the unbalanced shape of the first peak in the H–C function from this work differs significantly from the data of the previous MD study. The first coordination shell of the H atom, whose radius is equal to 7 Å (first minimum), contains ~ 9 CCl_4 molecules. However, the average number of the nearest molecules to the H atom, calculated up to the first maximum (4.4 Å), is ~ 2, and up to the intermediate point (5.15 Å) between first maximum and minimum, is ~ 4. Finally, the overall features of the H–C and Cl(a)–C functions reveal the existence of a structured cavity around each HCl molecule. Of course, this result may be explained in terms of the potential model employed in the present study.

The lower limit of this cavity is formed from the Cl(b) atoms nearest to the HCl. At this state, information regarding this average local structure may be obtained from the behavior of the atom–atom Cl(a)–Cl(b) and H–Cl(b) PCFs, presented in Fig. 1c. The Cl(a)–Cl(b) function is sharper peaked than the other PCFs of the system. This sharp peak is located at a significantly shorter distance (3.88 Å) than the first peak in the other functions. Moreover, the coordination number up to the first minimum in this function is ~ 13 and up to the first maximum is ~ 3 Cl(b) atoms. This number indicates that on average a maximum of 3 Cl(b) atoms attach to the Cl(a) atom of each HCl molecule.

In contrast to the Cl(a)–Cl(b) PCF, the H–Cl(b) PCF shows a more complicated behavior. From Fig. 1c and Table 5 we can see that this function shows a characteristic short-range local structure around the H atom. This behavior is quite different compared with corresponding results reported in the work of Idrissi et al. As we can see from this figure, the H–Cl(b) correlation exhibits a broad plateau between 2.7 and 3.6 Å followed by a broad peak located at 4.8 Å. Integration of the first peak of this function up to the minimum (7 Å) and up to the maximum (4.9 Å) yields 36 and 11 Cl(b) neighbor atoms, respectively. This result is in accordance with the average number of CCl_4 molecules (~ 9) around the H atom obtained up to the minimum of the H–C PCF (see Table 5).

Additional insight into the short local structure between H and the Cl(b) atoms can be gained by examining the observed shoulder in this function. For example, the appearance of the first peak in the Cl(a)–Cl(b) PCF at greater distance than the position of the shoulder in the H–Cl(b) function indi-

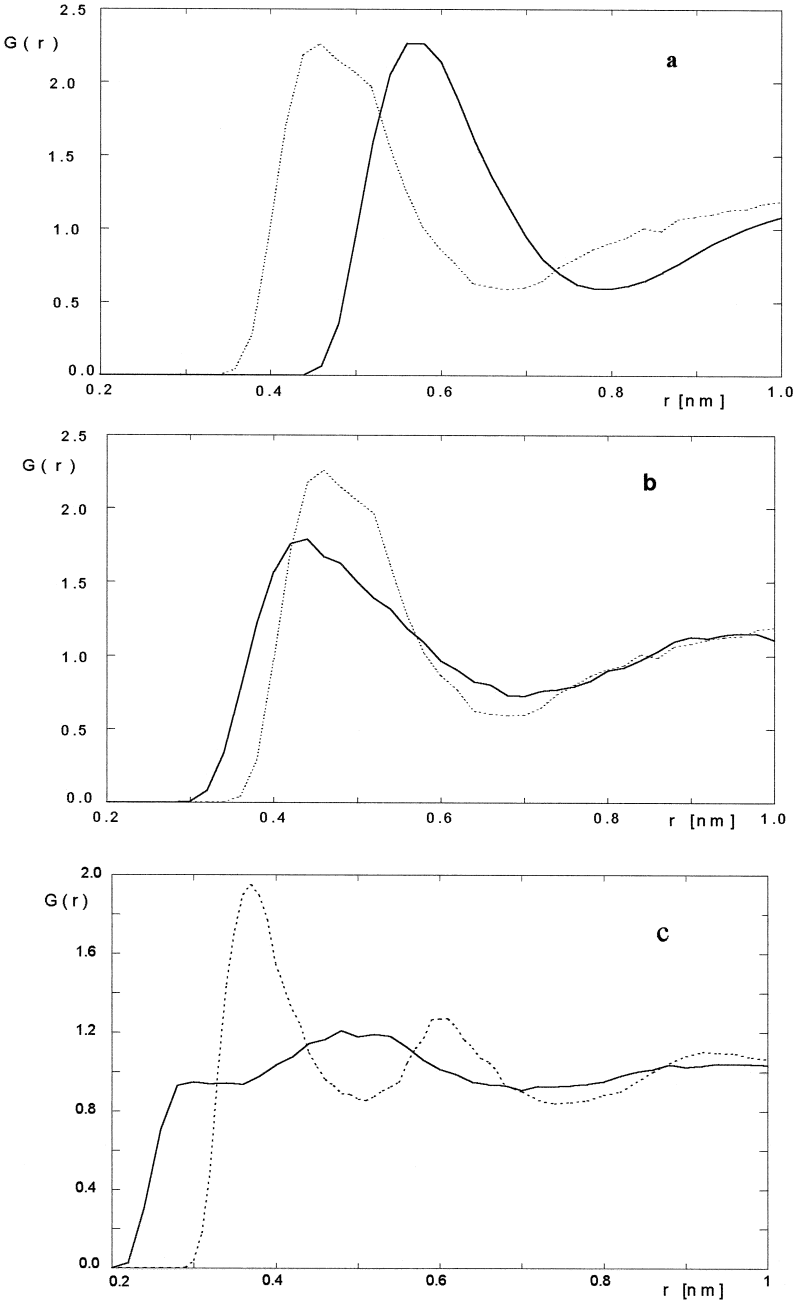

Fig. 1. Center of mass and site–site pair distribution functions $G(r)$ (a = HCl, b = CCl_4): (a) ——— = $G_{b-b}(r)$, · · · · · · = $G_{a-b}(r)$; (b) ——— = $G_{H(a)-C(b)}(r)$; · · · · · · = $G_{Cl(a)-C}(r)$; and (c) ——— = $G_{H-Cl(b)}(r)$, · · · · · · = $G_{Cl(a)-Cl(b)}(r)$.

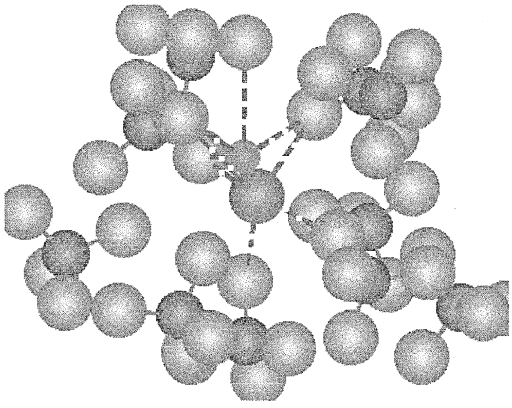

Fig. 2. A snapshot of the HCl cavity surrounded by the CCl_4 solvent molecules. The six Cl(b) atoms nearest to the HCl are shown with dashed line.

cates that, a small number of Cl(b) atoms are closer to the H atom than to the Cl(a) end of the HCl molecule. The number of Cl(b) atoms up to the right-hand limit of this shoulder (3.64 Å) is ~ 3.

Consequently, by taking into account the results of the procedure applied above, one may conclude that a relatively small number of Cl(b) atoms are in contact with the HCl molecule and correspond to what we call the solute cavity. It is found that on average the HCl cavity is formed by a maximum of six Cl(b) atoms. This finding may be correlated with previous X-ray scattering results of liquid CCl_4 [44]. In this experimental study Narten et al. proposed a successful lattice model of the average structure of this liquid. According to this model the arrangement of the molecules produces cavities which are approximately octahedral with six Cl atoms at the corners. In Fig. 2, a snapshot of the HCl cavity from the present study is shown. By inspecting this figure we see clearly that the observed HCl cavity is constructed by six Cl(b) atoms which are indicated with dashed bond lines between them and the two atoms of HCl. We also observe that this cavity is very irregular at a microscopic scale.

3.3. Dynamicical properties

In studying the dynamical properties of the molecular system, it is convenient to calculate and analyze the appropriate time correlation functions (TCFs).

3.3.1. Translational motion

We first studied the single-molecule translatioanal motion of the two components in the solution. The appropriate TCFs are the COM linear velocity auto-correlation functions (VACFs) $C_{\mathrm{u}}^{a}(t)$ and $C_{\mathrm{u}}^{b}(t)$. These ACFs are illustrated in Fig. 3a and the calculated correlation time corresponding to the VACF of the HCl molecules is given in Table 4. The curves in this figure show the following qualitative behavior. The VACF of the CCl_4 molecules first goes through a shallow negative minimum (in less than 0.45 ps) and then converges to zero after ~ 1.5 ps. On the other hand, the VACF of the solute molecules goes rapidly to zero (in less than 0.2 ps) and shows a deep anticorrelation region with a minimum of -0.2 at 0.3 ps. Obviously, the deep negative region in the VACF of HCl lower the value of the integral of this VACF. This denotes the greatness of the perturbation of the HCl translational motion due to the cage solvent molecules. Note also that the recoil on the cage walls is reflecting in the negative value of the VACF $C_{\mathrm{u}}^{a}(t)$ around 0.3 ps. This time interval may be characterized as the mean time of flight of the HCl between collisions with the cage walls.

In order to obtain some information about the force field acting on the COM of the solute and solvent molecules constructed from the surrounding molecules, we have calculated the COM total force auto-correlation functions (FACFs) $C_{\mathrm{F}}(t)$. Fig. 3b shows these results from which it is easy to see that the $C_{\mathrm{F}}^{a}(t)$ decays faster than the $C_{\mathrm{F}}^{b}(t)$. It is interesting to note furthermore that the HCl $C_{\mathrm{F}}(t)$ decays faster than the corresponding linear velocity ACF. This means that the total force acting on the HCl from the solvent molecules changes in direction at a relatively short time interval more frequently than the solute linear velocity.

3.3.2. Rotational motion

To shed some light on the rotational dynamics of the HCl and CCl_4 molecules in the solution, we have calculated the most important ACFs of the torque $C_{\mathrm{T}}(t)$, the angular velocity $C_{\omega}(t)$ and the first- and second-order Legendre reorientational ACFs C_L (L

$= 1, 2$) of the unit vector along the molecular axis of HCl:

$$C_1(t) = \langle \hat{u}_i(0) \cdot \hat{u}_i(t) \rangle, \quad (3)$$

$$C_2(t) = \frac{1}{2} \left\langle 3 |\hat{u}_i(0) \cdot \hat{u}_i(t)|^2 - 1 \right\rangle. \quad (4)$$

The angular velocity and the torque ACFs of the HCl and CCl_4 molecules are shown in Fig. 3c and d, respectively. The corresponding correlation times are selected in Table 4. In the case of the torque ACFs the results show the following behavior. The time dependence of the torque ACF of the CCl_4 exhibits a negative minimum with a depth of about -3.80 around 0.26 ps and then approaches zero after ~ 0.6 ps. As we can see, this function follows a different course compared to the torque ACF of HCl. In fact, the ACF of HCl decreases very fast up to 0.05 ps and exhibits a minimum of -0.2 around 0.09 ps. This function relaxes to zero at very short time of 0.2 ps. Note also that this correlation decreases faster than the total force ACF of HCl.

More insight into the nature of the rotational motion of the HCl molecule may be obtained from the angular velocity ACFs $C_\omega(t)$ of HCl. In fact, the function $C_\omega(t)$ is not directly accessible by optical spectroscopy or magnetic resonance. For this reason a direct comparison with experiment is not possible. However, results about this ACF from computer simulations of model liquids are generally very usuful in statistical mechanical theories. From Fig. 3c, the $C_\omega(t)$ ACF of CCl_4 exhibits a very slight negative minimum located at 0.5 ps. This function relaxes to zero at relatively long times and exhibits a behavior typical of molecules with low torque whose

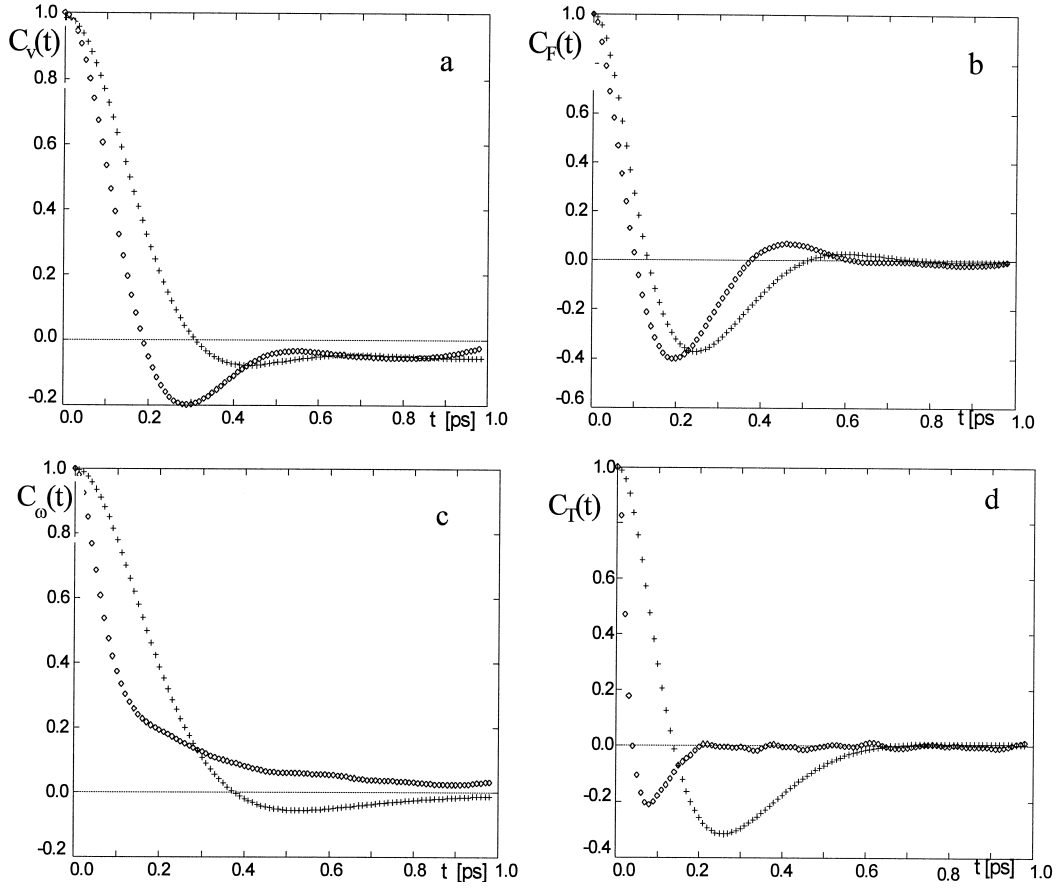

Fig. 3. Time autocorrelation functions obtained from this MD study (+ + + = CCl_4; ◇◇◇ = HCl).

rotational motion is weakly damped. In contrast to the CCl_4 ACF, the $C_\omega(t)$ of the HCl molecule does not exhibit a negative portion. This ACF decreases very fast up to 0.1 ps and after this time relaxes very slowly to zero. A similar behavior for this ACF has been obtained in a previous MD study of pure liquid HCl at 300 K. It means that on the average the angular velocity of the HCl molecule does not describe large alterations of its directions. A simple qualitative explanation of this can be given in terms of the dynamical behavior of the solute–solvent cavity. The HCl molecule is encaged by relatively heavy neighbors. Thus, the solute performs some rotational motion during the time domain it takes the system

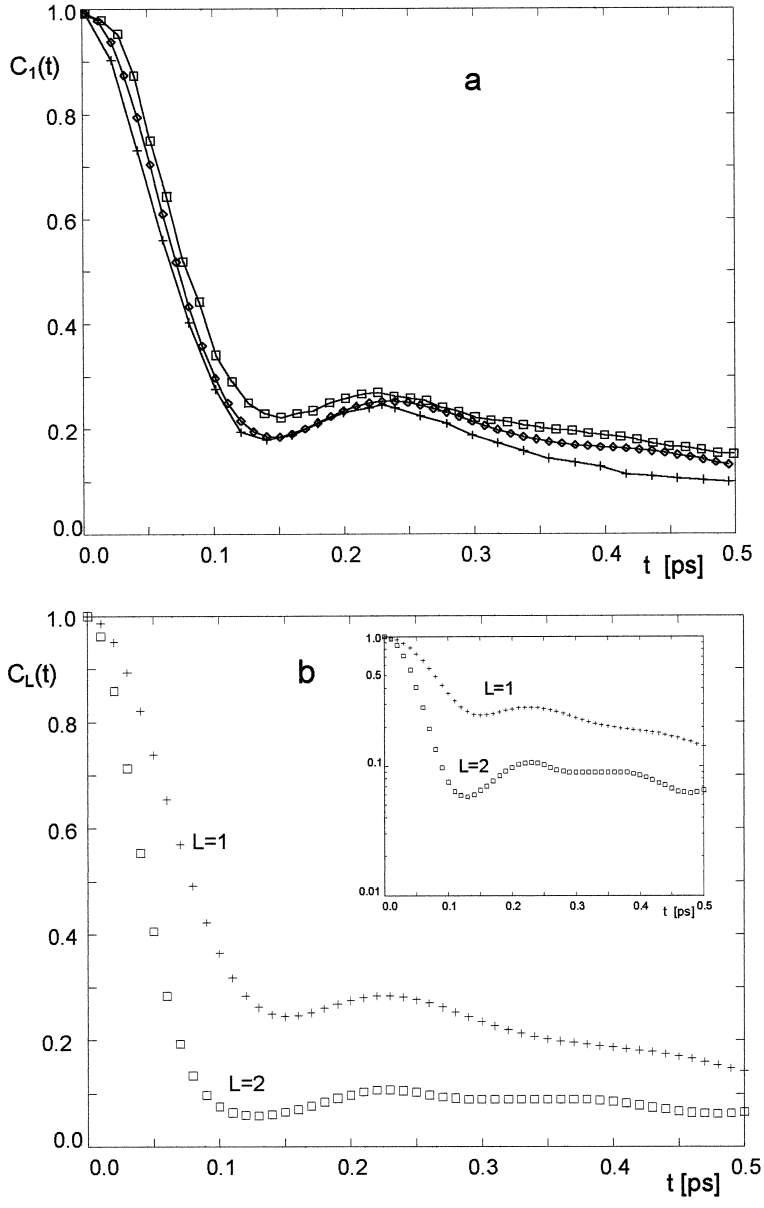

Fig. 4. First- and second-order reorientational ACFs of HCl in liquid CCl_4: (a) + + + = exp. from [3], ◇◇◇ = MD (this work); □ □ □ = exp. from [27]; and (b) $C_1(t)$ and $C_2(t)$ RACFs from this work. The inset shows the corresponding semilogarithmic plots.

solute-surrounding solvents to relax. In this time interval collisions between the solute and the cavity walls occur and interrupt the rotational motion. The period between successive wall-to-wall collision seems to be relatively short for an almost free rotation of HCl. This is in accordance with the short time behavior of the AVACF up to 0.1 ps. Therefore, we may conclude that the HCl rotates freely through a much smaller angle than 90° up to this time. After this time the AVACF reflects some collective rotational diffusion of HCl. This characteristic librational type motion of the HCl molecule in CCl_4 gives rise to a shoulder in the reorientation correlation functions $C_L(t)$ $(L = 1, 2)$ [45–47]. This feature has been observed in the calculated $C_1(t)$ and $C_2(t)$ RACFs from the present MD study.

Another point of great interest in the present treatment is to check on how well our proposed intermolecular potential predicts the experimentally accessible reorientational dynamics of HCl in CCl_4. As mentioned in Section 1, the reorientational dynamics of HCl in CCl_4 have been investigated by IR and FIR spectroscopic techniques in the past. Following the procedure described in Ref. [48] and by neglecting possible contribution of the induced dipole moments in the total dipole moment of the sample, we have calculated the corresponding to the IR band RACF $C_1(t)$ of HCl in the solution. Before proceeding further, we would like to discuss the available experimental results reported in two previous IR studies [3,27] of this solution at similar thermodynamic state. In fact, we first observe that the $C_1(t)$ ACFs of HCl and DCl in CCl_4 reported in Ref. [3] are similar with the $C_1(t)$ ACFs of DCl and HCl in CCl_4 reported in Ref. [27], respectively. At this stage, it is appropriate to point out that the origin of the observed discrepancy is due to a typographical error in the caption to fig. 4 in Ref. [27]. Concretely, the identification of the ACFs for HCl and DCl in the caption to this figure were interchanged [49]. Consequently, it becomes evident from the above discussion that we must compare our MD $C_1(t)$ ACF of HCl in CCl_4 with the corresponding function of HCl from [3], or with the ACF of DCl from [27]. It has been done in Fig. 4a from which we observe a quite satisfactory agreement between the experimental and simulated first-order RACFs. Moreover, from the Table 4 we see that the calculated MD τ_1 correlation time (0.19 ps) is in quite good agreement with the experimental one. This finding reveals the accuracy of our proposed potential model to describe the intermolecular forces in this molecular system and to predict successfully the rotational dynamics of the solute molecule in details. In addition, one may conclude that the origin of the observed submaximum in the experimental IR $C_1(t)$ RACF may be clearly attributed to the damped librational mode of HCl and not to the induction effects between solute and solvent molecules.

Finally, Fig. 4b shows the two RACFs and the inset their corresponding semilogarithmic plots. As expected, the $C_2(t)$ function decays faster than the $C_1(t)$. However, both functions relax very slowly to zero showing a collective reorientational behavior. As in the case of the $C_1(t)$ ACF, the $C_2(t)$ function exhibits a free rotator behavior at times up to 0.09 ps. Also, this function shows a slight minimum following by a submaximum at almost the same time position as in the $C_1(t)$ function.

4. Summary and conclusions

In the present paper, a molecular dynamics simulation study of the HCl/CC_4 solution has been performed in order to investigate the local intermolecular structure and the dynamics of the solute molecule in this molecular system. The results obtained may be summarized as follows:

In the framework of this treatment a new optimized effective potential model for this solution is proposed. Special attention has been paid to the solute–solvent interactions. It is found that these interactions may be approximated by a site–site exp $-$ 6, plus electrostatic terms, pair-additive potential model.

The thermodynamic results obtained are found to be in quite satisfactory agreement with experiment. The self-diffusion coefficients of the component molecules in the solution were calculated and the results obtained were found to be realistic. Also, the rms torque and force acting on the solute molecule have been obtained. We found that the rms torque from this study is reasonable compared to the experimental one.

The local intermolecular structure of HCl in this liquid has been obtained and analyzed in terms of the COM–COM and of the site–site pair distribution functions. The analysis of these functions reveals the existence of a structured cavity around the solute molecule constructed by a maximum of six Cl atoms from the CCl_4 solvent molecules nearest to the HCl.

The translational and rotational dynamics of the solute molecule have been extensively studied in terms of the most appropriate ACFs. The simulated and experimental $C_1(t)$ RACFs, obtained from the band lineshape of the IR vibration–rotation spectra, have been compared. The comparison shows that the minimum and submaximum of the experimental RACF is quantitatively reproduced. Generally, the potential model proposed here yields quite good agreement at both short and long times between experimental and MD $C_1(t)$ RACFs. On the other hand, the $C_2(t)$ RACF is not available in the literature. Consequently, a direct comparison of the simulated function with experiment is impossible at the present time. However, the time dependence of this correlation shows the expected behavior compared to the first-order RACF. Finally, it seems reliable that the employed potential model offers the possibility to study this solution further. Work on other interesting properties of this system is in progress.

Acknowledgements

This work was carried out within the project No. 70/4/3349AU. The financial support of the University of Athens is gratefully acknowledged. The CPU time allocation on CONVEX C3820 of the Supercomputing Center of the University of Athens-Greece, is also gratefully acknowledged.

References

[1] W.G. Rothschild, J. Chem. Phys. 49 (1968) 2250.
[2] G. Birnbaum, W. Ho, Chem. Phys. Lett. 5 (1970) 334.
[3] B. Keller, F. Knenbuehl, Helv. Phys. Acta 45 (1972) 1127.
[4] J. Lascombe, M. Besnard, P.B. Caloine, J. Devaure, M. Perrot, in: J. Lascombe (Ed.), Molecular Motion in Liquids, D. Reidel, Dordrecht, 1974.
[5] C. Dreyfus, L. Berreby, E. Dayan, J. Vincent-Geisse, J. Chem. Phys. 68 (1978) 2630.
[6] S. Bratos, Tarjus, in: Molecular Liquids — Dynamics and Interactions, Proc. NATO (N. Atlantic Treaty Org.), ASI (Adv. Stud. Inst.) on Molecular Liquids, Florence, 1983, p.151.
[7] A.I. Burshtein, S.I. Temkin, Spectroscopy of Molecular Rotation in Gases and Liquids, Cambridge University Press, Cambridge, 1994.
[8] C. Hocheisel, J. Chem. Phys. 89 (1988) 7457.
[9] A. Medina, A. Calvo Hernandez, Velasco, J. Chem. Phys. 100 (1994) 252.
[10] J. Samios, D. Dellis, H. Stassen, Chem. Phys. 178 (1993) 83.
[11] A. Medina, A. Calvo Hernandez, J.M.M. Roco, S. Velasco, J. Mol. Liq. 70 (1996) 169.
[12] S. Bratos, J. Rios, Y. Guissani, J. Chem. Phys. 52 (1970) 439.
[13] S. Bratos, E. Marechal, Phys. Rev. A 4 (1971) 1078.
[14] A.K. Soper, P. Egelstaff, Mol. Phys. 42 (1981) 399.
[15] K. Krynicki, J.G. Powles, J. Magn. Reson. 6 (1972) 539.
[16] H. Shapiro, D. Sadoway, J. Phys. Chem. 100 (1996) 5956.
[17] S. Murand, A. Papaioannu, J.G. Powles, Mol. Phys. 56 (1980) 253.
[18] S. Murand, AIChE (Am. Inst. Chem. Eng.) J. 32 (1986) 1049.
[19] M.L. Klein, I.R. McDonald, Mol. Phys. 42 (1981) 293.
[20] I.R. McDonald, D.G. Bounds, M.K. Klein, Mol. Phys. 45 (1982) 521.
[21] C. Votaka, R. Alrichs, A. Geiger, J. Chem. Phys. 78 (1983) 6841.
[22] A. Laaksonen, P.O. Westlund, Mol. Phys. 73 (1991) 663.
[23] Y. Ohikubo, S. Ikawa, M. Kimura, Chem. Phys. Lett. 43 (1976) 138.
[24] S. Ikawa, K. Sato, M. Kimura, Chem. Phys. 47 (1980) 65.
[25] S. Ikawa, S. Yamazaki, M. Kimura, Chem. Phys. 51 (1980) 151.
[26] G. Turrell, J. Mol. Spectrosc. 19 (1978) 383.
[27] E.C. Mushayakarara, G. Turrell, Mol. Phys. 46 (1982) 991.
[28] J.P. Perchard, W.F. Murphy, H.J. Bernstein, Mol. Phys. 23 (1972) 499.
[29] T. Kato, Mol. Phys. 43 (1981) 161.
[30] Y.P. Kalmykov, J. McConnell, Physica A 193 (1993) 394.
[31] H. Mori, Prog. Theor. Phys. 33 (1965) 424.
[32] D. Forster, Hydrodynamic Fluctuations, Broken Symmetry and Correlation Functions, Benjamin, New York, 1975.
[33] A. Morita, S. Walker, J.H. Calderwood, J. Phys. D 9 (1976) 2485.
[34] A.I. Burshtein, J. McConnell, Physica A 157 (1989) 933.
[35] P. Carlier, G. Turrell, J. Mol. Struct. 174 (1988) 41.
[36] A. Idrissi, F. Sokolic, G. Turrell, J. Mol. Liq. 70 (1996) 215.
[37] O. Steinhauser, M. Neuman, Mol. Phys. 40 (1980) 115.
[38] I.R. McDonald, G.D. Bounds, M.L. Klein, Mol. Phys. 45 (1982) 521.
[39] C.G. Gray, K.E. Gubbins, Theory of Molecular Fluids Oxford University Press, Oxford, 1984.
[40] K. Hlavaty, Czech. Chem. Commun. 35 (1970) 2878.
[41] B.S. Harsted, E.S. Tmomsen, J. Chem. Thermodyn. 7 (1975) 369.
[42] M.A. Siddiqi, K. Lukas, J. Chem. Thermodyn. 15 (1981) 1181.

[43] G. Turrell, D. Leclerc, M. Aubin, E. Mushayakarara, J. Mol. Liq. 27 (1983) 37.
[44] A.H. Narten, M.D. Danford, H.A. Levy, J. Chem. Phys. 46 (1967) 4875.
[45] W. Haertl, H. Versmold, J. Chem. Soc., Faraday Trans. 2 79 (1983) 1143.
[46] R.W. Impey, P.A. Madden, I.R. McDonald, Mol. Phys. 46 (1982) 513.
[47] H.D. Dardy, V. Voltera, T.A. Litovitz, J. Chem. Phys. 62 (1973) 4491.
[48] D. Dellis, J. Samios, Chem. Phys. 192 (1995) 281.
[49] G. Turrell, private communication.